Out-of-well carrier screening in a strained $In_xGa_{1-x}N$/GaN multiple quantum well structure

Fei Chen and A. N. Cartwright
Department of Electrical Engineering, University at Buffalo, State University of New York, Buffalo, New York 14260, USA
(Received 10 June 2003; published 9 December 2003)

Steady state and time-resolved differential transmission spectroscopy in a strained $In_xGa_{1-x}N$/GaN multiple quantum well structure embedded within a *p-i-n* structure has been studied to identify the dominant screening mechanisms and measure the carrier sweep-out time. The results are consistent with a long-range out-of-well carrier screening where the photoexcited carriers escape the wells and separate, creating a space-charge field that induces an increase of the in-well field and shifts the excitonic transition to lower energies. A redshift of excitonic resonance under photoexcitation suggests that the direction of in-well field is opposite to that in the barriers due to the piezoelectric polarization in this strained $In_xGa_{1-x}N$ well. Compared with GaAs multiple quantum wells, a long carrier sweep-out time of 650 ps was observed in this structure.

DOI: 10.1103/PhysRevB.68.233304 PACS number(s): 78.67.De, 71.35.−y, 78.47.+p

Time-resolved differential transmission measurements on GaAs multiple quantum wells (MQW's) embedded within a *p-i-n* structure have shown that the photoexcited electron-hole pairs in the quantum well (QW) under the influence of the electric field escape the well and travel in opposite directions to produce a space-charge field which opposes the built-in field.[1–4] This out-of-well carrier screening mechanism, through the quantum-confined Stark effect (QCSE), shifts the excitonic resonance and modifies the absorption of the QW. Measurements of the change in the absorption as a function of time delay and wavelength provide a unique way to determine the dynamics of perpendicular carrier transport and carrier sweep-out times in *p-i*(MQW)-*n* structures.

It is well known that hexagonal wurtzite III-nitride semiconductors have pronounced piezoelectric constant.[5,6] For $In_xGa_{1-x}N$/GaN QW's, the strength of the in-well electric field generated by spontaneous polarization and piezoelectric polarization can be as large as several MV/cm. Several groups have attributed the blueshift of the photoluminescence peak energy in undoped $In_xGa_{1-x}N$/GaN QW's with increasing carrier injection to the reduction of the QCSE due to in-well carrier screening.[7,8] Furthermore, built-in electric fields due to the *p-n* junction are present in these *p-i*(MQW)-*n* structures. Therefore, it is of interest to determine if the dominant carrier screening mechanism is in-well or long range out-of-well in such structures. A clear understanding of these carrier dynamics can provide great value for the design and optimization of $In_xGa_{1-x}N$ based emitters as well as for the optimization of material growth conditions. More importantly, such a study is expected to determine the carrier sweep-out times and provide insight into the potential profile in the strained $In_xGa_{1-x}N$/GaN MQW's. In particular, the sweep-out rate, a key property that limits the response time of nitride based *p-i-n* photodetectors, can be determined.

In this Brief Report, we report experimental results on steady state and time-resolved differential transmission measurements of an $In_xGa_{1-x}N$/GaN *p-i*(MQW)-*n* structure at room temperature. The differential transmission spectra are used to identify the dominant screening mechanisms and simultaneously to estimate the spatial band potential profile. A redshift of excitonic resonance immediately following pulsed excitation and a carrier sweep-out time of 650 ps were observed, indicating that photoexcited carriers sweep out of the well and screen the entire MQW structure. The increase of the in-well field under photoexcitation indicates that the direction of the in-well field is opposite to that in the barriers due to the piezoelectric polarization in the strained $In_xGa_{1-x}N$ wells.

The sample described in this work was grown using metalorganic vapor phase epitaxy. Initially, a 4 μm thick GaN:Si layer was deposited on a *c*-face sapphire substrate. This layer was followed by the growth of ten periods of 7 nm thick GaN barriers and 2.5 nm thick $In_{0.2}Ga_{0.8}N$ wells. The last QW was capped with a GaN barrier region followed by a 0.2 μm thick GaN:Mg *p*-contact layer. In order to determine the magnitude of the field distribution, we solved the Poisson equation for a *p-i*(MQW)-*n* structure within the depletion approximation. Neglecting the screening effects of background carriers, the net electric field within the wells (barriers) E_w (E_b) is

$$E_w = \frac{V_{bi}}{N_w L_w + N_b L_b + L_d/2} - E_{piezo} \times \frac{N_b L_b + L_d/2}{N_w L_w + N_b L_b + L_d/2}, \tag{1}$$

$$E_b = \frac{V_{bi}}{N_w L_w + N_b L_b + L_d/2} + E_{piezo} \times \frac{N_w L_w}{N_w L_w + N_b L_b + L_d/2}, \tag{2}$$

where E_{piezo} is the piezoelectric field discontinuity between strained wells and unstrained barriers and V_{bi} is the built-in potential due to *p-n* junction. L_w (L_b), N_w (N_b), and L_d represent the well (barrier) width, the number of wells (barriers), and the depletion width, respectively. The electric field in the depletion region was assumed to be linearly varying from zero to the maximum value, which resulted in $L_d/2$ in the above equations. Based on the carrier concentrations, we estimated the built-in potential to be 3.4 V, which induces an average *p-n* field (first term in above equations) of 0.28 MV/cm. Using a method developed by Takeuchi *et al.*,[9] the piezoelectric field discontinuity between wells and barriers is calculated to be 1.6 MV/cm. Due to the negligible spontaneous field discontinuity of ~0.068 MV/cm between $In_{0.2}Ga_{0.8}N$ well and GaN barrier, the effect of spontaneous polarization was not included in our calculation.[10,11] There-

 ©2003 The American Physical Society

TABLE I. Expected dependence of the excitonic shift and the rise time of differential absorption signal on the band potential profile and screening mechanisms.

Potential profile	In-well field opposite to *p-n* field		In-well field parallel to *p-n* field	
Screening	In-well	Out-of-well	In-well	Out-of-well
Excitonic shift	Blue	Red	Blue	Blue
Rise time	Fast (<1 ps)	Slow (>10 ps)	Fast (<1 ps)	Slow (>10 ps)

fore, the net electric field (parallel to the *c* axis) is -0.99 MV/cm in the well and 0.61 MV/cm in the barrier.

The differential absorption spectra critically depend on the location of the carriers responsible for the screening and on the band structure. The expected responses are summarized in Table I. The exciton is blueshifted if the carriers remain in the well and screen the in-well field, regardless of the in-well field direction. In contrast, if the screening is dominated by carriers that sweep out of the wells and move to screen the entire MQW's, it will depend on the direction of the in-well electric field. If the in-well field is opposite to the *p-n* field as calculated, a redshift of the exciton is expected. If it is parallel, a blueshift is expected. The expected change of spatial band structure due to out-of-well screening is shown in Fig. 1(a). Moreover, the rise time of the differential absorption spectra reflects the build-up of the space charge due to the vertical motion of electrons and holes. This signature analysis provides another way to identify the screening mechanisms. The typical carrier sweep-out time in GaAs MQW's for out-of-well screening ranges from 10 ps to 400 ps at room temperature.[1,2] This is much longer than the carrier transient time (<1 ps) across the well during in-well screening process.

Initially, we performed steady state pump/probe differential transmission measurements on this sample by pumping with a continuous-wave (cw) Ar^+ laser (3.41 eV) and probing with a Xenon lamp at room temperature. Standard lock-in techniques were used to measure the difference in the probe transmission (ΔT) with and without the pump present as a function of probe wavelength. The differential absorption spectrum was then extracted from the differential transmission: $\Delta\alpha = -[\ln(1+\Delta T/T)]/d$,[4] where d is the combined thickness of the InGaN QW's. The inset graph of Fig. 1(b) shows the expected absorption with the pump off (solid line) and the pump on (dashed line) for excitonic redshifting, as well as the resulting differential absorption signature ($\Delta\alpha$). The absorption with the pump on is expected to redshift due to an increase of the in-well field caused by out-of-well carrier screening. Figure 1(b) shows the steady state change in absorption coefficient, $\Delta\alpha$, as a function of photon energy under a cw pump irradiance of 0.4 W/cm^2. Notice that the dominant features are a positive peak followed by a negative peak, characteristic of a redshift of the exciton and consistent with the expected change in absorption shown in the inset of Fig. 1(b). This spectral feature suggests that the in-well field is opposite to the *p-n* field in the band potential profile. Furthermore, the carriers would be expected to escape the wells to screen the *p-n* field, resulting in an increase of in-well field.

Subsequent to these steady state measurements, time-resolved differential transmission at room temperature was used to determine the carrier sweep-out time and the dynamics of out-of-well screening. For these measurements, a portion of the 250 kHz 800 nm laser pulses from the regenerative amplifier (REGA) was frequency doubled to 400 nm to serve as the pump source. The remaining output from the REGA was used to create a broadband white light continuum,[12] with spectral components from 370 nm to 1000 nm (1.24 eV to 3.35 eV), which served as the probe beam. The time delay of the probe beam with respect to the pump beam was tuned by a motor-controlled delay stage. The time resolution of this system was limited to ~300 fs due to the broadened pulse width of the frequency-doubled pulse and the white-light continuum. In this case, the probe beam was focused to an 80 μm diameter spot on the sample and the transmitted light was spectrally resolved using a spectrometer. The pump spot size was chosen to be 160 μm.

Pulsed excitation is able to generate a significant carrier density compared with cw measurements. The *p-n* field or

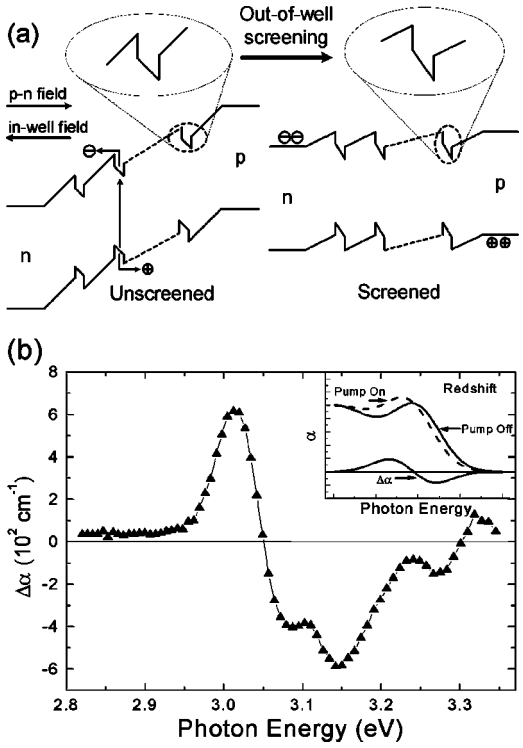

FIG. 1. (a) Expected change of the spatial band structure due to out-of-well screening and motion of the photoexcited carriers in a strained In_xGaN_{1-x}/GaN p-i(MQW)-n structure. (b) Steady state differential absorption spectra at room temperature under a pump irradiance of 0.4 W/cm^2. The inset graph is a schematic illustration of the expected change in absorption due to an excitonic redshift.

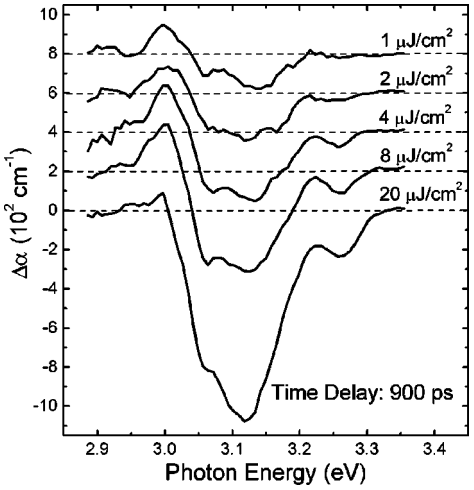

FIG. 2. Pump fluence dependent differential absorption spectra at a time delay of 900 ps at room temperature.

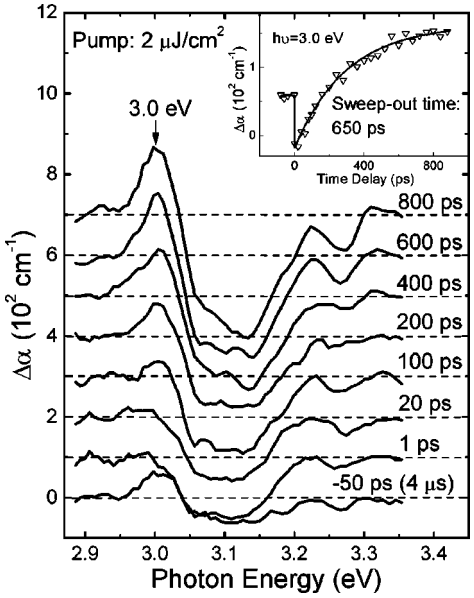

FIG. 3. Room temperature differential absorption spectra at various time delays under a pump fluence of 2 μJ/cm^2. The inset shows the time evolution of the $\Delta\alpha$ at 3.0 eV (hollow triangle). The solid line in the inset graph shows the results of a single exponential fit to the data.

in-well field may be completely screened in this case, and the absorption bleaching due to phase space filling could dominate the measured differential absorption spectra. Hence, it is essential to identify the individual contributions of field screening and absorption bleaching on the measured changes of absorption under various photoexcited carrier densities. Figure 2 shows the detailed pump fluence dependent differential absorption spectra at a time delay of 900 ps. This time delay ensures that enough carriers have escaped the wells and moved to screen the *p-n* field. At high pump fluence the *p-n* field is totally screened and a single negative peak due to absorption bleaching dominates the spectra. By contrast, at low pump fluence the observed spectral signature is consistent with the excitonic redshift (positive peak followed by a comparable negative peak) similar to the steady state spectra shown in Fig. 1(b). Consequently the differential absorption spectra is a combination of the absorption bleaching signal associated with the excess carriers remaining in the wells and the out-of-well screening signal associated with the carriers drift to the depletion regions to screen the entire MQW's. It is worth noting that the transition point (1.5 μJ/cm^2), between bleaching and screening, corresponds to the field strength of 0.29 MV/cm, which is in remarkably good agreement with the calculated value of the *p-n* field provided earlier.

Next, we temporally resolved the differential absorption spectra at low pump fluence. Figure 3 shows the differential absorption spectra versus time delay from -50 ps to 800 ps for a pump fluence of 2 μJ/cm^2. (The signal at the time delay of -50 ps also represents the accumulated signal at the time delay of 4 μs due to the 250 kHz pulse repetition.) Notice that immediately following pulsed excitation (1 ps time delay), a significant excitonic bleaching peak is observed, indicating that most of the carriers are still in the wells. As the carriers escape the wells and move to the edge of the MQW region to flatten the bands, the space charge field causes a graduate increase of the excitonic redshift (positive peak followed by a negative peak in the spectra) with increasing time delay as shown in Fig. 3. Additionally, the typical spectra, indicative of a redshift of the excitonic resonance, is still evident after 4 μs. This extreme prolongation of recovery time is caused by the large spatial separation between electrons and holes, where the electrons and holes separate across the entire MQW region into *n* doped and *p* doped regions, respectively. The reduced overlap integral of electron and hole wave functions leads to a significant decrease of recombination rate. In fact, the remaining carriers generated by the previous pulse, although not considerable, would screen the average *p-n* field and reduce the effects of sweep-out process when the next pulse comes.

The time evolution for the signal at an energy of 3.0 eV is shown in the inset graph of Fig. 3. Absorption bleaching causes an immediate drop in the signal at zero time delay. This drop is followed by a slow rise of the signal with time and the signal finally reaches a maximum value at around 800 ps. This rise time is indicative of the sweep-out time of carriers escaping the wells and drifting to the doped regions.[1,2] The sweep-out time, defined as the 10–90 % rise time of the differential absorption signal, was determined to be 650 ps.

For GaAs MQW systems, the carrier sweep-out process was investigated extensively and was suggested to be dominated by thermionic emission and/or various tunneling mechanisms such as thermally assisted tunneling,[2] escape tunneling through tilted barriers,[13] resonant tunneling,[14] or phonon-assisted tunneling.[15] Our calculations show that the thermionic emission times for both electrons and holes are much longer than the measured carrier sweep-out time, when we use the values of 6:4 as a ratio for conduction and valence band discontinuities.[16] For simplicity, here we only consider the carrier tunneling process. Hence, the sweep-out time τ_{so} is given by the sum of the tunneling escape time τ_{escape}, and the transit time τ_{tr} for the carriers to reach the doped regions: $\tau_{so}=\tau_{escape}+\tau_{tr}$.[15] The strength of tunneling can be deter-

mined by evaluating the rate of tunneling of an individual particle using the Wentzel-Kramers-Brillouin approximation[17–19]

$$\tau_{escape} \propto \frac{\hbar \pi}{\varepsilon_i} \exp\left(2 \times \int_0^W \left[\frac{2m_i}{\hbar^2} \times (V_b - eE_b z) \right]^{1/2} dz \right), \quad (3)$$

where $V_b - eE_b z$ is the barrier height as the carriers go through the GaN barrier region, m_i is the electron (hole) effective mass, and W represents the effective barrier thickness. In our calculations, electrons have much faster tunneling rate than holes due to their five times lighter effective mass, where the effective electron mass with a value of $0.2m_0$ was used. The tunneling times were estimated as 290 ps and 6.3 ns for electrons and holes, respectively, from Eq. (3). The experiment techniques used here generally measure the fastest escaping carriers. Hence, the calculated tunneling time for electrons, although shorter, is comparable to the measured sweep-out time. In fact, Eq. (3) is only valid for the sweep-out time for a particular well. Once the carriers escape for the well, some of them will be swept straight to the doped layers, but others will be scattered and recaptured by subsequent wells. Such recapture process may increase the effective sweep-out time. More importantly, it should be emphasized that because of the heavier carrier effective masses of GaN, the carrier sweep-out time (650 ps) measured here is relatively longer than that of GaAs MQW's. In addition, the opposite direction of the in-well field with respect to that in the barriers in this $In_xGa_{1-x}N$/GaN *p-i*(MQW)-*n* structure may increase the effective barrier thickness and barrier height, leading to a decrease of the sweep-out rate.[19] Such slow sweep-out rate is a disadvantage for applications of these $In_xGa_{1-x}N$ materials as photodetectors.

Another issue that needs to be clarified is the effects of the in-well screening on the measured differential absorption spectra. Generally, both in-well screening and out-of-well screening can occur. Huang *et al.* have observed the presence of the in-well screening at early time delays in the piezoelectric GaAs MQW's, but they showed the out-of-well screening response was significantly larger than the in-well screening response.[20] The absolute strength of the in-well screening is dependent on the carrier density, charge separation, and the well width. As the width of the well decreases, a reduction of the in-well screening effect would be expected as a result of a decrease of charge separation. The self-consistent calculations solving the Poisson equation and Schrödinger equation in the narrow QW, have verified that the induced blueshift of the exciton due to in-well screening is negligible when compared with out-of-well screening,[21] even in the case where significant numbers of carriers are still in the well. As expected, the signature of excitonic blueshifting due to in-well screening for a 2.5 nm $In_xGa_{1-x}N$ well here is not readily observed, even at very short times. Besides, the presence of absorption bleaching would obscure and further decrease the effects of the in-well screening.

Thus the experimental results presented here may be explained as follows. Initially, the femtosecond pulse generates electron-hole pairs that escape the well and drift to the opposite sides of the MQW region under the influence of the *p-n* field. Thus, the built-in field is screened and the intrinsic in-well piezoelectric field increases. This drift of carriers will continue until the resulting space charge fields have effectively screened the built-in *p-i-n* field and the bands are roughly flat across the MQW region.

In conclusion, the photoexcited carrier dynamics in an $In_xGa_{1-x}N$/GaN *p-i*(MQW)-*n* structure have been studied by steady state and time-resolved differential transmission measurements. The results have provided convincing evidence that the out-of-well carrier screening is the dominant screening mechanism in this sample. This out-of-well screening induces an increase of in-well field and a redshift of the excitonic resonance. The estimated average *p-n* field at the transition point between out-of-well screening and excitonic bleaching is consistent with the estimated theoretical value. A carrier sweep-out time was observed as 650 ps in this structure.

This work was supported by the National Science Foundation CAREER Award, NSF No. 9733720, under the direction of Dr. Filbert Bartoli, and the Office of Naval Research Young Investigator Program Award No. N00014-00-1-0508 under the direction of Dr. Colin Wood.

[1] G. Livescu *et al.*, Phys. Rev. Lett. **63**, 438 (1989).
[2] A. M. Fox *et al.*, IEEE J. Quantum Electron. **27**, 2281 (1991).
[3] D. S. McCallum *et al.*, IEEE J. Quantum Electron. **30**, 2790 (1994).
[4] A. N. Cartwright *et al.*, J. Appl. Phys. **73**, 7767 (1993).
[5] F. Bernardini and V. Fiorentini, Phys. Rev. B **57**, R9427 (1998).
[6] F. Bernardini and V. Fiorentini, Phys. Status Solidi B **216**, 392 (1999).
[7] T. Kuroda and A. Tackeuchi, J. Appl. Phys. **92**, 3071 (2002).
[8] P. Riblet *et al.*, Appl. Phys. Lett. **75**, 2241 (1999).
[9] T. Takeuchi *et al.*, Jpn. J. Appl. Phys., Part 2 **36**, L382 (1997).
[10] F. Bernardini and V. Fiorentini, Phys. Rev. B **56**, R10024 (1997).
[11] V. Fiorentini *et al.*, Phys. Rev. B **60**, 8849 (1999).
[12] C. Nagura *et al.*, Appl. Opt. **41**, 3735 (2002).
[13] T. B. Norris *et al.*, Appl. Phys. Lett. **56**, 2031 (1989).
[14] K. Leo *et al.*, Appl. Phys. Lett. **56**, 2031 (1990).
[15] J. Feldmann *et al.*, Appl. Phys. Lett. **59**, 66 (1991).
[16] Ch. Manz *et al.*, Appl. Phys. Lett. **74**, 3993 (1999).
[17] K. Kohler *et al.*, Phys. Rev. B **38**, 5496 (1988).
[18] L. I. Schiff, *Quantum Mechanics* (McGraw-Hill, Tokyo, 1986).
[19] Y. D. Jho *et al.*, Phys. Rev. B **66**, 035334 (2002).
[20] X. R. Huang *et al.*, Appl. Phys. Lett. **67**, 950 (1995).
[21] M. Livingstone *et al.*, Appl. Phys. Lett. **65**, 2771 (1994).